Search for the top quark in the hadronic decay channel

J. M. Benlloch
Massachusetts Institute of Technology, Cambridge, Massachusetts 02139

N. Wainer and W. T. Giele
Fermi National Accelerator Laboratory, P.O. Box 500, Batavia, Illinois 60510

(Received 19 April 1993)

The possibility of discovering the top quark and measuring its mass at the Fermilab Tevatron collider is studied for the pure hadronic decay channel, that is, the six jet final state. The most important aspects of a generic detector relevant for this study are included. By requiring tagging of a b-quark jet and applying cuts on the sphericity, aplanarity, and summed scalar transverse energy of the jets we obtain an acceptable signal-to-background ratio. In order to reduce the uncertainty in the measured three jet invariant mass distribution due to energy smearing, kinematical fit techniques are used. With the above methods we conclude that a top quark with a mass up to 180 GeV can be observed in the hadronic decay mode at the Tevatron with an integrated luminosity of 100 pb^{-1}.

PACS number(s): 13.85.Ni, 12.38.Bx, 13.87.Ce, 14.80.Dq

I. INTRODUCTION

With the discovery of the top quark the fermion sector of the three generation standard model will be completed. Apart from its necessity for theoretical consistency of the standard model the existence of the top quark is inferred by several measurements, for example, the forward backward asymmetry in $Z \rightarrow b\bar{b}$ at the CERN e^+e^- collider LEP [1] and the absence of flavor-changing neutral currents [2].

Compared to the other quarks the top quark is very heavy. The current direct search lower mass limit is 91 GeV [3], set by the Collider Detector at Fermilab (CDF) Collaboration at the Tevatron $p\bar{p}$ collider.

Indirect limits on the top-quark mass can be estimated by comparing all available data with electroweak calculations which include the oblique corrections [4]. This method assumes that no new physics is present which might effect the oblique corrections. With the precision measurements of the Z boson mass and the strong-coupling constant at LEP, one obtains a top-quark mass of $m_t = 155 \pm 30$ GeV [5]. The main source of error is caused by the uncertainty in the W boson mass measurement and the unknown Higgs boson mass. With the main injector upgrade at the Fermilab Tevatron, resulting in an integrated luminosity well over 1000 pb^{-1}, a good measurement of both the W boson mass and the top-quark mass will be possible. This will test the consistency of the standard model very accurately and put indirect limits on the Higgs boson mass.

Because of the high top-quark mass the weak decays occur faster than the scale over which strong interactions form bound-state mesons [6]. The top quark is expected to decay into a W boson and a b quark assuming no deviations from the standard model. With the two possible decay modes of the W boson the top quark is in principle observable in two final states.

(1) The top quark decays into jets, associated with the hadronic decay of the W boson. The b-quark jet can be tagged and the W boson will mainly decay into two jets with an invariant mass equal to the W mass. This gives the final state of three jets of which one is a b-quark jet.

(2) The top quark decays into one b-quark jet, a charged lepton and a neutrino resulting from the leptonic decay of the W boson.

The dominant top-quark production at the Fermilab Tevatron in the mass range of interest is through the process $p\bar{p} \rightarrow t\bar{t}$. The cross section is a steeply falling function of the top-quark mass varying from 30 pb at 120 GeV to 5 pb at 190 GeV [7]. The Tevatron is expected to deliver an integrated luminosity of 25 pb^{-1} in 1993 and 100 pb^{-1} in 1994 for each of the two experiments CDF and D0. The discovery range with the expected luminosity will cover the indirect top-quark mass limits obtained from the standard-model constraints. The produced top-quark pairs have three possible decay channels, giving three different search methods: (1) the dilepton final state with two b-quark jets, having a branching ratio of $\frac{4}{81}$ or 5%; (2) the single lepton plus four jets final state, having a branching ratio $\frac{24}{81}$ or 30%; (3) the six jet final state having the largest branching ratio of $\frac{36}{81}$ or 44%. The remaining 21% of the top-quark decays are associated with τ lepton final states which have not been taken into account. Also detector efficiencies have not been taken into account.

Apart from the largest branching ratio, the measurement of the top-quark mass in the six jet decay mode has another important advantage over measuring the mass in leptonic decays. In leptonic events one neutrino is present for each semileptonic decay. This neutrino escapes the detector and it is not measured. In six jet top-quark events the full event is reconstructed.

In the top-quark search so far only the channels containing at least one lepton have been considered. This results mainly from the fact that it is relatively easy to trigger on a hard lepton in an experiment. Also most

phenomenological papers with emphasis on the top-quark search at $p\bar{p}$ colliders [8] do not consider the six jet signal. This is because the signal is completely overwhelmed by a huge QCD jet background which is of the order of 100 nb, as shown in Fig. 1. However, the use of the 44% of the cross section in the fully hadronic channel and the larger acceptance of the detector for jets is quite tempting.

With the use of a silicon microvertex detector (see, for example, Ref. [9]) and soft lepton identification, an efficiency of the order of 50% can be obtained for tagging a b-quark jet. Requiring at least one b-tagged jet leads to a reduction factor of 100 for the QCD background [10] (see Fig. 1). Note that for high-momentum b quarks, the tagging efficiency increases. A heavy top quark produces higher transverse momentum (P_T) b jets, increasing the b-tagging efficiency significantly.

In this paper we explore the feasibility of top-quark search in events with a six jet topology of which at least one is tagged as a b-quark jet. A typical detector response for jets is simulated to obtain the usual reduction in cross section.

II. MONTE CARLO SAMPLES

To generate the multijet events from top-quark decays we use the calculation of Ref. [11]. This calculation gives the exact tree-level result for this process and includes all the spin correlations between the produced jets, nonzero b-quark masses and finite width W boson.

To generate the QCD background we have used the Monte Carlo program NJETS which is based on the calculations of Ref. [12]. This program contains the exact tree-level matrix elements for all processes up to and including five jets. If one increases the number of jets beyond five the processes containing more than three quark pairs are not included. These processes are expected to give negligible contributions to the total jet cross section.

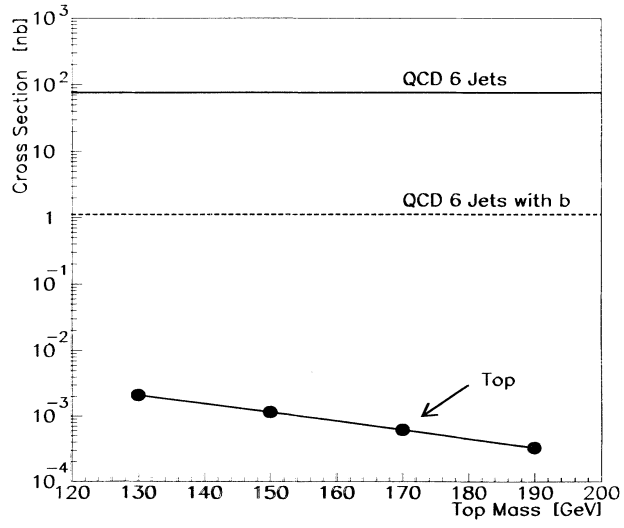

FIG. 1. The $t\bar{t}\rightarrow$ six jets cross section for different top-quark masses. Also shown the QCD prediction for six jets production (solid) and the QCD prediction for six jets production with at least one b-quark (dashed).

Tight cuts have to be applied in order for the leading-order approximation to be valid. With the used jet definitions no large higher-order corrections are expected for the observables relevant in this study. The computation of the matrix elements for six jets is very slow and the use of approximations in the Monte Carlo simulation is imperative if one wants to obtain reasonable statistics for the generated distributions. In Ref. [12], an approximation was used to calculate the six jet cross section. This method uses the infrared reduction techniques developed in Ref. [13] to approximate the six jet production from lower multiplicity jet calculations. This approximation has been studied extensively in the literature and proved to be valid if one considers the shape of the distributions. The total cross section, however, is systematically overestimated. The cross section is overestimated by a factor of approximately 1.2 for the cuts used in this paper.

In this study we evaluate the strong coupling constant and the structure functions at an energy scale equal to the average transverse momentum of the jets. The used structure functions are the Martin-Roberts-Stirling set B [MRS(B)] parametrization of Ref. [14]. The effects of changing the scale and parton distribution functions has been investigated in Ref. [10] and estimated to be of the order of 50%. Note that this uncertainty is much larger than the uncertainty resulting from the infrared reduction approximation.

The events in NJETS are generated with the unit weight event generator of Ref. [15]. Each accepted event is then assigned a weight proportional to the matrix element. However because of the steeply falling distribution of the transverse momentum of the partons, this procedure is very inefficient and produces large weight fluctuations in the generated events. When trying to get events with equal weight by a weighting rejection algorithm it becomes impracticable. To overcome this problem we have increased the efficiency by the use of important sampling in the inclusive P_T distribution of the jets. This gives a significant improvement in the efficiency. Details are given in Appendix A.

We simulated detector effects by convoluting the jet energies obtained from the generators with a function that describes the CDF detector jet resolution [16]. This function can be approximated by the expressions

$$\frac{\sigma_{E_T}}{E_T}\sim\frac{80\%}{\sqrt{E_T}} \quad \text{for } 10\ \text{GeV}<E_T<35\ \text{GeV}\ ,$$
$$\sigma_{E_T}\sim 0.1\times E_T \quad \text{for } E_T>35\ \text{GeV}\ . \tag{1}$$

In Fig. 2 the missing transverse energy significance is shown, defined as

$$S=\left|\sum \mathbf{P}_T\right| \Big/ \sqrt{\sum |\mathbf{P}_T|}\ ,$$

where $\mathbf{P}_T$ is the transverse momentum of the jet. The significance S is a measure of detector resolution. S is larger for poorer detector resolutions.

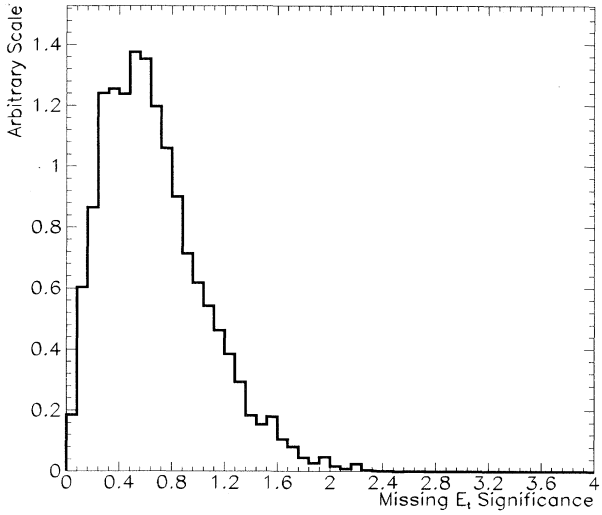

FIG. 2. Missing E_T distribution as an indication of the assumed detector performance in the simulation.

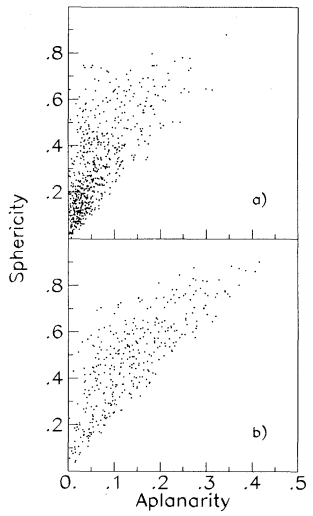

FIG. 3. Sphericity vs aplanarity distributions (using the cuts described in the text) (a) for the QCD prediction and (b) for top-quark events with a mass of 130 GeV.

In the subsequent top-quark analysis we will apply the following cuts: a six jet final state; a transverse momentum cut on the jets of $P_T^{\text{jets}} > 10$ GeV; a jet pseudorapidity cut $|\eta^{\text{jets}}| < 2.5$, with $\eta = \ln(\cot\theta/2)$ and θ being the polar angle of the jet;

$$\Delta R_{\text{jet-jet}} = \sqrt{\Delta\phi^2 + \Delta\eta^2} > 1$$

cut, where $\Delta\phi$ is the azimuthal angle between the jets and $\Delta\eta$ the pseudorapidity difference of the jets. Apart from the last cut, which mimics a realistic jet-clustering algorithm, the applied cuts are efficient because the top-quark decay produces high-momentum jets in the central region.

III. KINEMATICAL VARIABLES

Intuitively one expects the jets from the hadronic top-quark decay to be kinematically different than QCD multijet production. The jets in the top-quark events come in two pairs of three jets each resulting from a heavy top quark. This will produce, in general, high-momentum, central, and well-separated jets. The jets will tend to be spherically distributed in the center-of-mass frame of the collision. The background events on the other hand are bremsstrahlung jets which implies the jets tend to be soft, collinear, and forward. This will make the jets far less spherically distributed.

In order to quantify the above event topology we introduce two types of cuts.

(1) We use cuts on the event shape distributions of the six jets. The simplest way to characterize the event topology is to calculate the sphericity tensor $M_{\alpha\beta} = \sum_j P_{j\alpha} P_{j\beta}$ in the center-of-mass frame of the event, where α and β are the Cartesian components of the three-dimensional momentum P and the sum is over all jets in the event. The three normalized eigenvalues are ordered such that $Q_1 \le Q_2 \le Q_3$. From this we calculate the sphericity and aplanarity of the event which are defined by

$$S = \tfrac{3}{2}(Q_1 + Q_2), \quad A = \tfrac{3}{2} Q_1 \ . \tag{2}$$

In Fig. 3 the sphericity vs aplanarity is plotted for both the background and the top-quark signal with a top-quark mass of 130 GeV. The result is typical for a top-quark mass up to 190 GeV. By examining Fig. 3 we apply the following cuts: sphericity > 0.2; aplanarity > 0.05.

(2) Another useful quantity is the sum of all the jet transverse energies in the event. For the top-quark pair production the summed transverse energies will peak

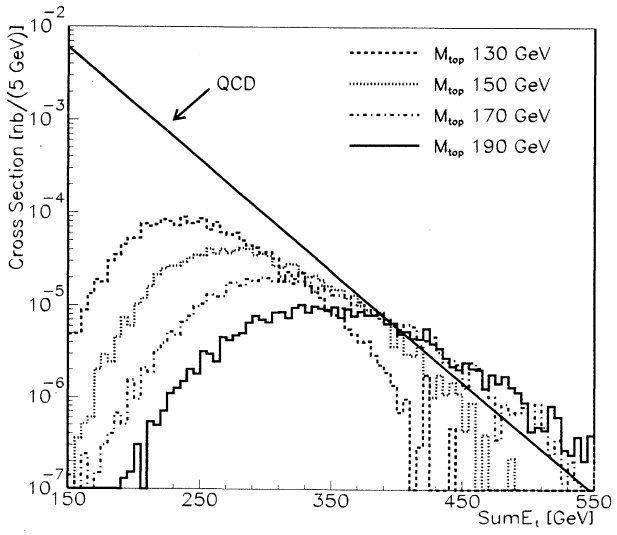

FIG. 4. Differential cross section as a function of summed E_T of the jets in the event for various top-quark masses and QCD background, after applying b-tagging and the sphericity and aplanarity cuts.

around a value slightly lower than twice the top-quark mass. On the other hand, the QCD background is a steeply falling function of the summed transverse energy. In Fig. 4 the differential cross section of the summed transverse energy is shown. For the final analysis we apply a cut of 210 GeV on the summed transverse energies. This reduces the QCD background substantially.

The combination of the above cuts has for a top-quark mass of 130 GeV an efficiency of 70%. This efficiency increases for heavier top-quark masses. So, although the cross section for top-quark production decreases as a function of the mass, this is partly compensated by an increase in efficiency.

IV. CONSTRAINED FITS

The experimental precision in jet energy measurements is typically of the order of 10%. This uncertainty is reflected in the top-quark mass which has to be reconstructed from the six jet final state.

In order to improve the precision of the jet energy measurements we can use properties of top-quark production and decay. That is the apparently independent jet measurements can be correlated by constraints which arise from the top-quark process.

The first constraint comes from the hadronic W boson decay. We can use the condition that the two jet invariant mass is equal to the W boson mass. Having two hadronic W boson decays, we constrain two pairs of jet energies.

Because the decay width of the top quark is ~ 1 GeV, much smaller than the experimental mass resolution, one can implement an additional kinematical event constraint. Namely, that the top quark and top antiquark have the same mass giving a constraint on the remaining two jets in the event. Intuitively, one expects that the transverse momentum balance of the top quarks would give an additional constraint. However, for a realistic experimental environment the transverse momentum balance cannot be imposed.

The least-squares-fit method used requires an error matrix relating the measured components of the jet four-vector. In order to simplify the analysis we assume a massless jet and neglect the error on the jet direction with respect to the error on the measured jet energy. For example, at the CDF detector jets are measured with an energy accuracy in the best case of $\sim 10\%$ and direction accuracy of 1°–2° [17]. With this approximation the error matrix is diagonal.

Using the least-squares formalism the kinematical constraint resulting from the W boson decay leads to the following expression for the χ^2 of the two jet energies E_u and E_d:

$$\chi^2_W = \left[\frac{E_u^m - E_u}{\sigma E_u}\right]^2 + \left[\frac{E_d^m - E_d}{\sigma E_d}\right]^2 \tag{3}$$

with the constraint

$$K_W \equiv \frac{M_W^2}{2(1-\cos\theta_{ud})} = E_u E_d \tag{4}$$

where the measured jet energies are given by E_u^m and E_d^m with their respective errors σ_{E_u} and σ_{E_d}, M_W is the W vector boson mass and θ_{ud} is the opening angle between the two jets.

Using Eq. (4) the minimization of the χ^2_W function can be reduced to the condition

$$\frac{\partial \chi^2_W}{\partial E_u} = 0 \tag{5}$$

leading to a quartic equation in E_u:

$$\sigma^2_{E_d} E_u^4 - \sigma^2_{E_d} E_u^m E_u^3 + K_W \sigma^2_{E_u} E_d^m E_u - \sigma^2_{E_u} K_W^2 = 0 \ . \tag{6}$$

The equation has four roots: two real and two imaginary. Only one of the roots gives the real and positive physical solution.

We already have at least one of the jets tagged as a b-quark jet. This leaves us with at most fifteen possible combinations of the remaining five jets to be assigned to the decay products of the two W bosons. We choose the combination which has the minimal sum of the two independent χ^2_W's. With this procedure we (1) select the most likely assignment of the W boson decay jets giving the two W boson momenta and (2) improve the jet energy measurements using Eqs. (3) and (5).

There are still two possibilities for associating the W bosons to the b-quark jets. With the condition that the top-quark masses are equal, $m_t^2 = m_{\bar{t}}^2$, we can constrain the b-quark jet energies and associate the jets with the corresponding W boson to reconstruct a single top-quark momentum. The equal top-quark mass condition gives

$$E_{W^+} E_b - \sqrt{E^2_{W^+} - M^2_W}\,\sqrt{E_b^2 - M_b^2}\cos\theta_{W^+ b} = E_{W^-} E_{\bar{b}} - \sqrt{E^2_{W^-} - M^2_W}\,\sqrt{E_{\bar{b}}^2 - M_b^2}\cos\theta_{W^- \bar{b}} \ , \tag{7}$$

where the W boson energies E_{W^+} and E_{W^-} are given by Eqs. (3) and (5) and $\theta_{W^+ b}$ and $\theta_{W^- \bar{b}}$ are the opening angles between the W's and their associated b jets.

The χ^2_t is given by

$$\chi^2_t = \left[\frac{E_b^m - E_b}{\sigma_{E_b}}\right]^2 + \left[\frac{E_{\bar{b}}^m - E_{\bar{b}}}{\sigma_{E_{\bar{b}}}}\right]^2 \ . \tag{8}$$

We have a χ^2_t value for each of the two assignments. The smallest of the two χ^2_t is selected to give the most likely combination of the b-quark jet and W boson momentum which reconstructs the top-quark momentum.

After we reconstructed the event using the above-described procedure and determined the energy of the jets using the constraints we apply additional cuts to the explicit values of χ^2_W and χ^2_t.

We require the sum of the χ^2_W of the two W's to be less than 3.5 and χ^2_t to be less than 6. With these cuts the total efficiency for top-quark signal becomes of the order of 50%. The signal-to-background ratio becomes of the order of one.

In 50% of the cases the right combination of jets is chosen to the top and top antiquark by applying these

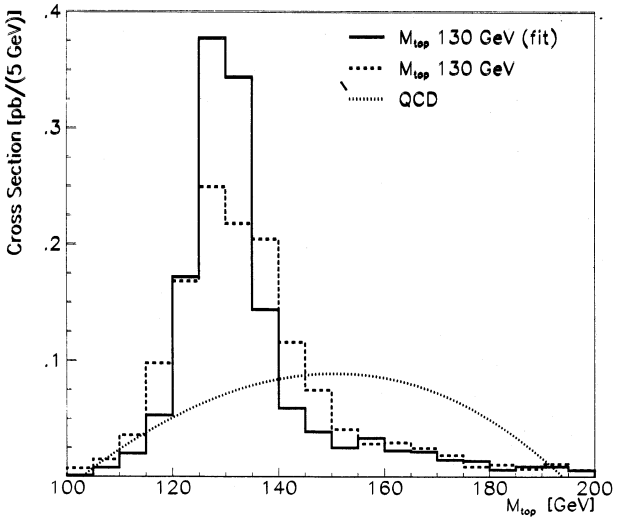

FIG. 5. Background (dotted) and signal for the top-quark mass measurement before (dashed) and after (solid) applying the kinematical constraints, for a top-quark mass of 130 GeV.

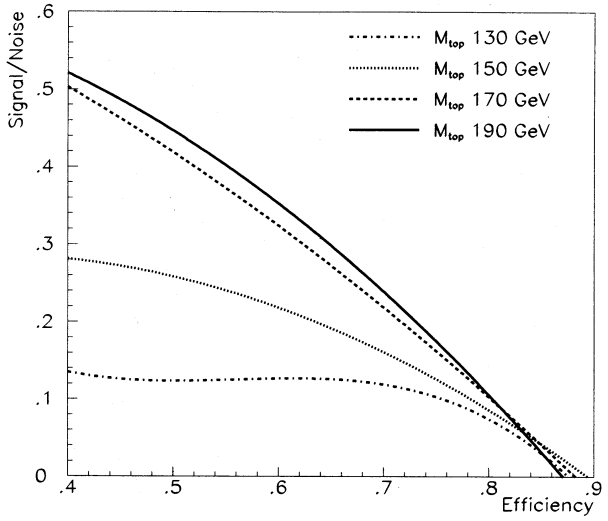

FIG. 6. Signal-to-background ratio as a function of the top-quark detection efficiency for the following values of the top-quark mass: 130, 150, 170, and 190 GeV.

cuts, that is all six jets are correctly assigned. In the remaining wrongly reconstructed events 40% of the cases still give the right top-quark mass because we still assign the correct three jets coming from its decay. So in 70% of the cases we reconstruct the correct top-quark mass.

The improvement on the top-quark mass measurement after applying the kinematical constraints is shown in Fig. 5 for a top-quark mass of 130 GeV. The mass resolution is improved by a factor of ~ 2 compared to the three jet invariant mass distribution without any kinematical constraints. In the region of the top-quark mass peak the signal-to- background ratio is ~ 4.

V. RESULTS AND CONCLUSIONS

The search for the top quark in the hadronic decay mode involves three steps.

(1) Tagging one of the b-quark jets.

(2) Explore kinematical differences between top-quark events and QCD background. In particular, the sum of the transverse energies of the jets is a useful quantity to select top-quark events. Its discriminating power increases with top-quark mass.

(3) Apply constrained kinematical fits to obtain the three jet invariant mass peak.

In Fig. 6 we show the signal-to-background ratio as a function of the efficiency for top-quark detection for different top-quark masses. The efficiency is normalized to the number of events which have six jets, and a b-quark tagged. The points in the signal to background vs efficiency plane were obtained by varying the cut on the ΣP_T over the jets, while keeping the sphericity and aplanarity cuts fixed at 0.2 and 0.05, respectively. The efficiency of these event shape cuts does not vary significantly with top-quark mass. The curves plotted are polynomial fits to these points. It is interesting to note that for a given efficiency the signal to noise (background) increases dramatically with the top-quark mass.

The introduction of the kinematical constraints not only reduces the background but also improves substantially the measurement of the top-quark mass by making it less dependent on the relative energy corrections of different parts of the detector. Using the kinematical constraints the signal-to-noise ratio in the four bins under the mass peak in Fig. 5 is 4:1.

In Fig. 7 we summarize our results by plotting the needed luminosity in order to produce a top-quark mass peak in the three jet invariant mass distribution with significance of three standard deviations. Both the ideal case and a more realistic scenario are plotted. In the

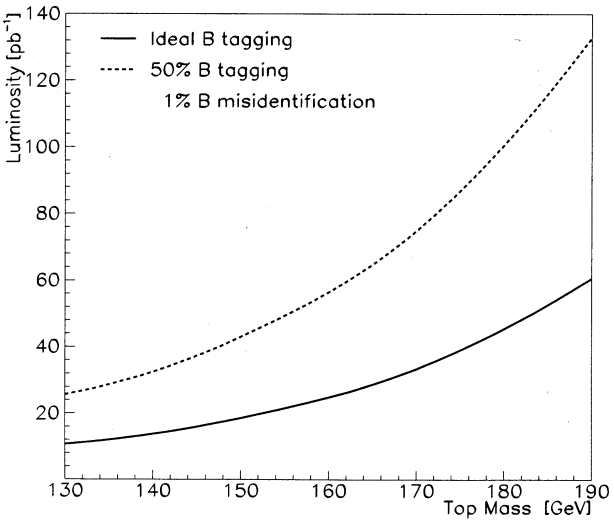

FIG. 7. Luminosity required for getting a three sigma signal to background ratio as a function of the top-quark mass for the cases of a perfect b-tagging and a more realistic b-tagging efficiency of 50% combined with a 1% fake rate.

ideal case we assume that at least one b-quark jet is tagged with 100% efficiency. The more realistic case assumes that only 50% of the top-quark events are tagged with b tagging. Also a 1% misidentification rate of the b-tagging algorithm is assumed. This misidentification rate increases the background rate by a factor of 2. As the top-quark mass becomes heavier, its production cross section decreases requiring more luminosity to discover the top quark. From Fig. 7 it is readily seen that if the Tevatron delivers 100 pb^{-1} by the end of 1994, top-quark masses up to ~ 180 GeV can be detected using this method.

In conclusion, the implementation of kinematical cuts, b-quark tagging, and kinematical fits allows the all hadronic decay channel to be added as a valuable method for the top-quark search, especially for heavy top-quark masses. Furthermore, in the hadronic six jet channel all the decay products of the top quark are measured making this channel ideal to determine the top-quark mass accurately. Also determining the top-quark mass in all three decay channels will be a necessary test to ensure standard-model branching ratios.

APPENDIX: IMPORTANT SAMPLING

When using the NJETS code [12] for high number of jets as was needed in this analysis one encounters a problem using the built-in phase-space generator RAMBO [15]. This phase-space generator produces the final state momenta according to flat phase space. This means that the n-jet momenta p_i are generated according to

$$d\Phi_n(P;p_1,\ldots,p_n)=\delta^4\left[P-\sum_{i=1}^{n}p_i\right]\prod_{i=1}^{n}\frac{d^3p_i}{(2\pi)^3 2E_i} \quad \text{(A1)}$$

with unit weight. This is very convenient for general purpose applications. However, for our purposes we would need to generate too many events in order to reduce the integration errors to an acceptable level.

The main source of the weight fluctuations is the sharp increase of the jet cross section at small transverse energy of the jet, $E_t^{\rm jet}$. This is associated with the soft singularity in the matrix elements. The singularity is not compensated by the phase-space generator, giving a large increase in the cross-section weight for events generated with a small transverse energy. The proper way to treat such a numerical instability is using the method of important sampling (see, e.g., Ref. [18]). In this method we generate the $E_t^{\rm jet}$ according to its differential cross section. Instead of the increase in weight for small $E_t^{\rm jet}$, one obtains unit weight for the $E_t^{\rm jet}$ spectrum. By inspection of the average differential $E_t^{\rm jet}$ distribution we model this by

$$\frac{d\sigma}{dE_t^{\rm jet}}=A\frac{\exp(-\alpha E_t^{\rm jet})}{E_t^{\rm jet}} , \quad \text{(A2)}$$

where A is an irrelevant overall normalization factor and α an adjustable parameter which will depend on the jet multiplicity and used jet cuts.

We convert the integration over the momentum p_i to an integration over the transverse energy E_t, rapidity η and azimuthal angle ϕ of the jet. The jet four-vector becomes

$$\begin{aligned} p&=(E,p_x,p_y,p_z)\\ &=E_t(\cosh(\eta),\cos(\phi),\sin(\phi),\sinh(\eta)) . \end{aligned} \quad \text{(A3)}$$

The Monte Carlo integration over a jet momentum where the events are generated according to Eq. (A2) is given by

$$\begin{aligned} \int\frac{d^3p}{(2\pi)^3 2E}\frac{\exp(-\alpha E_t^{\rm jet})}{E_t^{\rm jet}}&=\int_{-\eta^{\max}}^{\eta^{\max}}d\eta\int_0^{2\pi}d\phi\int_{E_t^{\min}}^{E_t^{\max}}dE_t\frac{1}{2}E_t\frac{\exp(-\alpha E_t^{\rm jet})}{E_t^{\rm jet}}\\ &=W^{E_t}\int_{-\eta^{\max}}^{\eta^{\max}}d\eta\int_0^{2\pi}d\phi\int_0^1 dr , \end{aligned} \quad \text{(A4)}$$

where

$$W^{E_t}=\frac{1}{\alpha}[\exp(-\alpha E_t^{\min})-\exp(-\alpha E_t^{\max})] \quad \text{(A5)}$$

and the $E_t^{\rm jet}$ is given by

$$E_t^{\rm jet}(r)=-\frac{1}{\alpha}\ln[r\exp(-\alpha E_t^{\min})+(1-r)\exp(-\alpha E_t^{\max})] . \quad \text{(A6)}$$

The integrals over rapidity and azimuthal angle are done trivially.

In the phase-space generator we generate for the n-jet events $(n-1)$ jet momenta using the important sampling. The transverse momentum of the last jet is then constrained by transverse momentum balance. The rapidity of the last jet is still unconstrained and determines the boost of the system. However, the momenta fractions x_1 and x_2 are now constrained and determined by the final-state jet momenta. The phase-space integration now becomes

$$\int d\Phi_n(P;p_1,\ldots,p_n)=\left[\prod_{i=1}^{n-1}w_i\int_0^1 dr_i^{\phi}dr_i^{\eta}dr_i^{E_t}\right]w_n\int_0^1 dr_n^{\eta}\left[\prod_{i=1}^{n-1}E_t^{\rm jet}(r_i^{E_t})\exp\left[\alpha E_t^{\rm jet}(r_i^{E_t})\right]\right] , \quad \text{(A7)}$$

where the transverse energy of jet i is given by $E_t^{\rm jet}(r_i^E)$ of Eq. (A6). The rapidity and azimuthal angle of momentum i are, respectively,

$$\eta(r_i^{\eta})=\eta^{\max}(2r_i^{\eta}-1)\ , \tag{A8}$$

$$\phi(r_i^{\phi})=2\pi r_i^{\phi} \tag{A9}$$

and the weights w_i are given by

$$\begin{aligned} w_i &= 4\pi\eta^{\max}W^{E_t}(r_i^{E_t}) \quad \text{for } i\le n-1\ , \\ w_n &= 2\eta^{\max}\ . \end{aligned} \tag{A10}$$

Note that we have to demand the condition that the reconstructed parton fractions should satisfy the condition $0\le x_{1,2}\le 1$. Events which fail these cuts have to be rejected. One could in principle include this constraint in the boundaries of the rapidity generation of jet n. However, the number of generated events failing this constraint is small, not justifying a complicated calculation of the boundary.

Finally the program VEGAS [19] was used to optimize the $3n-2$ integration variables of Eq. (A7).

[1] ALEPH Collaboration, D. Decamp *et al.*, Phys. Lett. B **263**, 325 (1991); DELPHI Collaboration, P. Abreu *et al.*, *ibid.* **276**, 536 (1992); L3 Collaboration, O. Adriani *et al.*, *ibid.* **292**, 454 (1992).

[2] CLEO Collaboration, P. Avery *et al.*, Phys. Rev. Lett. **53**, 1309 (1984); CLEO Collaboration, A. Bean *et al.*, Phys. Rev. D **35**, 3533 (1987).

[3] CDF Collaboration, F. Abe *et al.*, Phys. Rev. Lett. **68**, 447 (1992).

[4] D. Kennedy and B. W. Lynn, Nucl. Phys. **B322**, 1 (1989).

[5] G. Altarelli, in *Electroweak Interactions and Unified Theories,* Proceedings of the 27th Rencontre de Moriond, Les Arcs, France, 1992, edited by J. Tran Thanh Van (Editions Frontieres, Gif-sur-Yvette, 1993).

[6] V. Fadin, V. Khoze, and T. Sjostrand, Z. Phys. C **48**, 613 (1990); T. Sjostrand and P. Zerwas, in e^+e^- *Collisions at 500 GeV: The Physics Potential,* Hamburg, Germany, 1991, edited by P. Zerwas (DESY Report No. 92-123, Hamburg, 1992).

[7] P. Nason, S. Dawson, and R. K. Ellis, Nucl. Phys. **B303**, 607 (1988).

[8] W. T. Giele and W. J. Stirling, Nucl. Phys. **B343**, 14 (1990); H. Baer, V. Barger, J. Ohnemus, and R. J. N. Phillips, Phys. Rev. D **42**, 54 (1990); R. K. Ellis and S. Parke, *ibid.* **46**, 3785 (1992); F. A. Berends, J. B. Tausk, and W. T. Giele, *ibid.* **47**, 2746 (1993).

[9] F. Bedeschi *et al.*, in *Proceedings of the 26th International Conference on High Energy Physics,* Dallas, Texas, 1992, edited by J. Sanford, AIP Conf. Proc. No. 272 (AIP, New York, 1993).

[10] W. T. Giele, D. A. Kosower, and H. Kuijf, in *QCD '90,* Proceedings of the International Workshop, Montpellier, France, 1990, edited by S. Narison [Nucl. Phys. B (Proc. Suppl.) **23B**, 22 (1991)].

[11] R. Kleiss and W. J. Stirling, Z. Phys. C **40**, 419 (1988).

[12] H. Kuijf, Leiden University, Doctoral thesis, 1991; F. A. Berends and H. Kuijf, Nucl. Phys. **B353**, 59 (1991).

[13] C. J. Maxwell, Phys. Lett. B **192**, 190 (1987); Nucl. Phys. **B316**, 321 (1989).

[14] A. D. Martin, R. G. Roberts, and W. J. Stirling, Phys. Rev. D **37**, 1161 (1988).

[15] R. Kleiss, W. J. Stirling, and S. D. Ellis, Comput. Phys. Commun. **40**, 359 (1986).

[16] S. Behrends (private communication); CDF Collaboration, F. Abe *et al.*, Phys. Rev. Lett. **68**, 1104 (1992).

[17] CDF Collaboration, F. Abe *et al.*, Phys. Rev. Lett. **70**, 713 (1993).

[18] R. Kleiss, Leiden University, Doctoral thesis, 1982 (unpublished).

[19] G. P. Lepage, Cornell Report No. CLNS-80/447, 1980 (unpublished).